Applied Physics Letters

Nanowire crystals of tantalum nitride grown in ammonium halide fluxes at high pressures

Cite as: Appl. Phys. Lett. **116**, 123102 (2020); https://doi.org/10.1063/1.5140856
Submitted: 02 December 2019 . Accepted: 07 March 2020 . Published Online: 24 March 2020

Nico Alexander Gaida, Takuya Sasaki, Zheng Liu, Ken Niwa, Masaki Hirozawa, Tetsu Ohsuna, and Masashi Hasegawa

Applied Physics Letters ARTICLE scitation.org/journal/apl

Nanowire crystals of tantalum nitride grown in ammonium halide fluxes at high pressures

Cite as: Appl. Phys. Lett. **116**, 123102 (2020); doi: 10.1063/1.5140856
Submitted: 2 December 2019 · Accepted: 7 March 2020 ·
Published Online: 24 March 2020

Nico Alexander Gaida,[1,2,a)] Takuya Sasaki,[1] Zheng Liu,[3] Ken Niwa,[1] Masaki Hirozawa,[1] Tetsu Ohsuna,[1] and Masashi Hasegawa[1]

AFFILIATIONS

[1]Department of Materials Physics, Nagoya University, Furo-cho, Chikusa-ku, Nagoya 464-8603, Japan
[2]Venture Business Laboratory, Nagoya University, Furo-cho, Chikusa-ku, Nagoya 464-8603, Japan
[3]National Institute of Advanced Industrial Science and Technology (AIST), Shimo-shidami, Moriyama-ku, Nagoya 463-8560, Japan

[a)]**Author to whom correspondence should be addressed**: gaida@mp.pse.nagoya-u.ac.jp. **Tel.:** +81-52-789-5515

ABSTRACT

Nanowire crystals of a tantalum nitride phase have been grown from epsilon-tantalum nitride and ammonium halide precursors at high pressures exceeding several gigapascals. Synchrotron x-ray diffraction and Transmission Electron Microscopy (TEM) observations revealed that they had crystallized in an unreported hexagonal structure with lattice parameters of $a = 3.050(1)$ Å and $c = 2.909(2)$ Å. The one-dimensional growth orientation was along the crystallographic [001] direction. Scanning TEM–EDX elemental analyses showed that the nanowire crystals were composed of tantalum and nitrogen with small amounts of oxygen. The presence of the melted ammonium halides combined with supercritical ammonia acting as a reactive flux at high pressure and temperature played a significant role in the nanowire crystal growth. Raman spectroscopy performed on several single crystal nanowires pointed toward metallic properties, and the temperature dependence of the magnetization measured by Superconducting Quantum Interference Device magnetometry suggested a superconducting transition about 6.2 K. The analysis of the compression behavior revealed an incompressible nature, and the bulk modulus was determined to be 363(6) GPa.

Metal nitrides, in particular, those of transition metals (TMs), have attracted remarkable attention in solid-state and applied physics in terms of ultra-high bulk modulus and high hardness,[1–4] superconductivity,[4–7] wide-bandgap semiconductors,[8] ferromagnetism,[9] and so on. Pressures in the gigapascal (GPa) range have played a crucial role in the development of TM nitrides[4] as they favor the unconventional N–N bonding in the crystal structures of TM nitrides. A number of TM nitrides and pernitrides, such as MoN,[10] MoN_2,[11–13] PtN_2,[2] Ta_2N_3,[14] Ta_3N_5,[15] Hf_3N_4,[16] Zr_3N_4,[17] FeN_2,[18,19] TiN_2,[20] RuN_2,[21] ReN_2,[22,23] W_2N_3,[24] and so on, have been discovered at high pressures. Furthermore, the crystal morphology often controls the functionality of crystalline materials because physical properties are sensitive to the shape of crystals and can be substantially improved by minimizing their dimensionality.[25,26] One-dimensional (1D) crystals (e.g., nanowire crystals) bear several advantages, such as a high surface-area-to-volume ratio, nearly perfect crystalline geometry, or high theoretical strength, which can significantly improve the electronic, optoelectronic, thermal, or mechanical characteristics.[27–31] However, growing metal nitride crystals with a 1D architecture under high pressure lies ahead. In general, crystals of 1D materials can be naturally grown with a highly anisotropic crystal morphology in an isotropic growth environment. For materials with higher crystal structural symmetry, the anisotropic growth must be induced by symmetry breaking in the nucleation step of the crystals.[27] Various strategies have been demonstrated for growing 1D materials, including vapor-liquid-solid (VLS), vapor–solid (VS), template-directed, or solvothermal growth.[27,31]

A flux method is one of the most established techniques for crystal growth and can be readily applied for extreme conditions of GPa-high pressure and high temperature (high P-T conditions).[32–34] In the present study, the flux technique has been employed to grow 1D nanowire crystals of TM nitrides. Ammonium halides (NH_4X with X = Cl, Br, I, F) seem to be appropriate flux candidates under high P–T conditions as presented for the high P–T synthesis of β-MNX (M = Zr, Hf; X = Br, I)[35] or MoN[36] crystals. Ammonium halides are convenient to handle, they are solid at ambient conditions and highly soluble in water, and thus, residuals can be easily removed. However,

the NH_4X behavior is still not entirely elucidated at extremely high P–T conditions.

In the present study, nanowire crystals (NWCs) of tantalum nitride were grown from Ta nitride and ammonium halide NH_4X (with X = Cl; I; Br; F) precursors at high pressure (1–5 GPa) and temperature (1000–1400 °C). Tantalum nitrides are considered to be attractive functional materials. For instance, NaCl-type TaN possesses superconductivity[37,38] and WC- and NaCl-type TaN and Ta_5N_6 have high bulk moduli, which are likely to be hard materials,[39] whereas Ta_3N_5 is an efficient photocatalyst for water splitting.[40,41] Beyond that, it has been recently proposed that WC-type TaN and NbN are topological semimetals, which provide an interesting type of point node, i.e., triply degenerate nodal points.[42] Although Ta nitrides show these interesting physical and chemical properties and some nano-sized 1D TaN crystals[40,41,43] have been reported, achieving their crystal growth in one crystallographic direction remains challenging.

For the crystal growth experiments, raw materials were homogeneously mixed according to the molar ratio of ε-TaN:NH_4X = 1:1 or 1:2 (with X = Cl; I; Br; F) in a glovebox operating in an argon atmosphere. High pressures were applied by the transformation of uniaxial forces of hydraulic presses into quasi-hydraulic pressure using a DIA-type multi-anvil press (Fig. S1). Recovered samples were identified by in-house x-ray diffraction (XRD, Rigaku Raxis-VII, Cu–Kα, λ = 1.5418 Å) and synchrotron XRD at the Aichi Synchrotron Radiation Center (BL2S1 and BL5S2, λ = 0.7499–0.9999 Å),[44] Aichi Science and Technology Foundation (Japan). Field-emission Scanning Electron Microscopy (SEM) operating at 10 kV (Hitachi S-4800) and Transmission Electron Microscopy (TEM) combined with selected area electron diffraction (SAED) by using a JEM-2100F operated at 200 kV provided details of the one-dimensional nature of the materials. The chemical composition was extracted by energy dispersive x-ray spectrometry (EDX) analyses at a scanning TEM (STEM) mode by using a JEM-ARM200F operated at 200 kV equipped with an SDD-EDX system. For further Raman scattering measurements, a finely focused laser with a monochromatic wavelength of 473 nm (<15 mW) was used as an excitation source. A large number of randomly arranged NWCs were analyzed with Superconducting Quantum Interference Device (SQUID) magnetometry (Quantum Design MPMS3). Samples were carefully prepared based on literature recommendations[45,46] for measurements of small samples with weak magnetic signals. Finally, the compression behavior was studied with high-pressure *in situ* synchrotron XRD by using a diamond anvil cell (DAC) at the Aichi Synchrotron Radiation Center (BL2S1, λ = 0.7499 Å).[44]

Figure 1 presents SEM images of NWCs obtained after 3 GPa and 1100 °C treatment of a homogenous mixture of ε-TaN ($P\bar{6}2m$) and NH_4Cl. The NWCs had high aspect ratios (length to diameter) of up to ~300 with diameters of ~40 to 200 nm and lengths of ~100 nm to in some cases more than ~50 μm depending on the respective wire. Some NWCs exhibited wave-like morphology and elemental mappings of these structures confirmed tantalum and nitrogen within them [Figs. 1(c) and 1(d)]. The largest NWCs were even visible under high magnifications with a light microscope and were significantly bent by a fine needle. In addition to the NWCs, numerous bulk crystals in a hexagonal shape were found in the samples synthesized at lower pressures (≤3 GPa).

To investigate pressure effects on the crystal growth, the synthesis pressure had been systematically changed. The number of NWCs

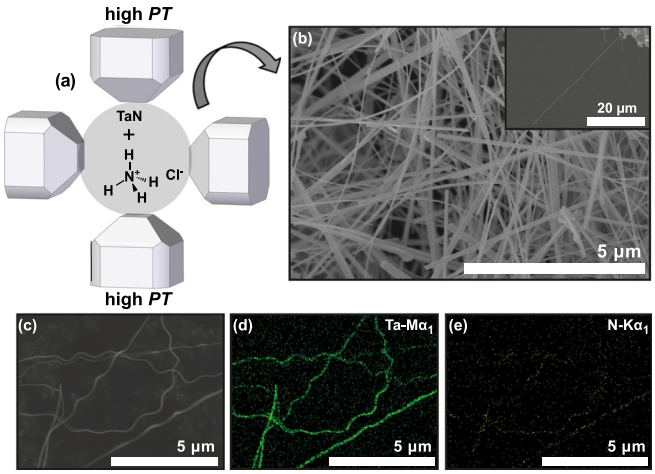

FIG. 1. (a) Schematic illustration of the high-pressure synthesis using TaN and NH_4Cl precursors. (b) A SEM image displays a "spider web" of NWCs after washing (inset: high-aspect ratio NWC). (c) SEM images of wave-like NWCs before washing. (d) and (e) Corresponding elemental mappings of tantalum and nitrogen (P, T = 3 GPa, 1100 °C).

steadily increased concomitant with the vanishing of hexagonal crystals with increasing pressure (Fig. S2), until almost solely NWCs were present in the recovered sample at 5 GPa and 1100 °C. These findings were consistent with synchrotron XRD patterns (Fig. 2) indicating the coexistence with hexagonal Ta_5N_6[47] or $Ta_5N_{6-x}O_x$[48] ($P6_3/mcm$) which most likely correspond to the hexagonal crystals in the samples synthesized at lower synthesis pressures (1–3 GPa). SEM-EDX measurements on these crystals detected small amounts of oxygen, suggesting a $Ta_5N_{6-x}O_x$ phase. The lattice constants of this hexagonal phase were calculated to be a = 5.179(1) Å and c = 10.361(2) Å, which are consistent with those reported in the literature.[48]

As the number of NWCs increased with growth pressure, several reflections assigned to the nanowires became more intense while the other reflections almost disappeared [Fig. 2(a)]. From these reflections, the crystal structure of the NWCs was solved to be hexagonal with

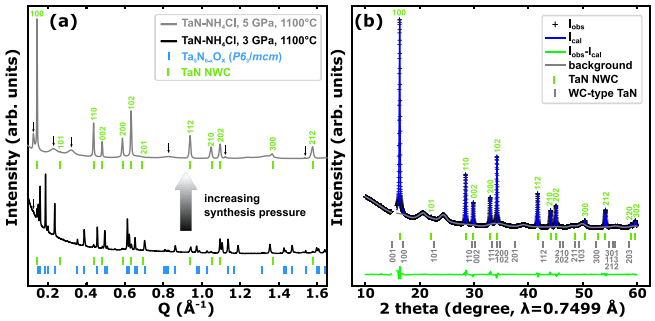

FIG. 2. (a) Synchrotron XRD pattern of the samples obtained from TaN–NH_4Cl after washing (P, T = 3 and 5 GPa, 1100 °C). Diffraction patterns were collected from several single NWCs isolated from the bulk agglomerate. The arrows mark unknown lower intense and broad reflections that might have been originated from monoclinic TaON.[49,50] (b) Le Bail refinement of the XRD pattern of the sample that is almost solely composed of nanowires.

lattice constants of $a = 3.050(1)$ Å and $c = 2.909(2)$ Å. These are very similar to those of synthesized WC-type TaN ($P\bar{6}m2$)[39,51] ($a = 2.933$–2.934 Å), $c = 2.880$–2.882 Å) and almost the same as theoretical values ($a = 2.913$–3.018 Å, $c = 2.862$–2.967 Å).[39] Since the observed reflections satisfied the diffraction conditions *hhl*: $l = 2n$ and *00l*: $l = 2n$, the space group was expected to be one of *P6cc* (No. 184), $P6_3mc$ (No. 186), $P\bar{6}2c$·(No. °190), *P6/mcc* (No. 192), or $P6_3/mmc$ (No. 194). A Le Bail refinement[52,53] [Fig. 2(b)] agreed well with the observed pattern confirming their hexagonal structure and Superflip[54] solved the $P6_3/mmc$ space group. These crystallographic data differed from those of reported TaN phases as well as from the space group of WC-type TaN as illustrated by the simulated reflections in Fig. 2(b) (compare Table S1). Accordingly, the NWCs were considered to be a Ta nitride phase that crystallizes in an unreported hexagonal structure.

With all these points in mind, several single NWCs were investigated using TEM and Raman spectroscopy to confirm and amplify the crystallographic details. Figure 3(a) displays a TEM micrograph of a NWC. From the tilting series of SAED patterns (Fig. S3) taken from the NWC, the sharp diffraction spots were able to be indexed by the lattice constants obtained from XRD. Growth orientation of the hexagonal NWCs was along the crystallographic [001] direction and STEM-EDX analyses indicated that the atomic compositional ratio of Ta:N:O was approximately 1:1:0.1–0.2 (Fig. S4), concluding an oxygen-doped TaN NWC phase, i.e., TaN(O). The oxygen-bearing phases have most likely resulted from the presence of oxygen in the reaction chamber. Oxygen might have been introduced by impurities in the starting material, as particularly NH_4Cl is hygroscopic and, therefore, could be contaminated with H_2O. Due to the small amounts of oxygen, the NWCs were referred to as oxygen-doped Ta nitride (TaN). No peaks were detected in the Raman measurement spectra recorded on several single NWCs [Fig. S5(a)]. Although no crystallographic information was obtained from the data, the absence of Raman signals marked a non-Raman active crystal structure (e.g., crystals, in which atoms occupy symmetry centers) or metallic characteristics.

Regarding the possible metallic nature and the matter of fact that TM nitrides often feature a superconducting transition,[4] a large number of NWCs were measured using a SQUID magnetometer. The sharp clear decrease in the zero-field cooling (ZFC) of the magnetization data

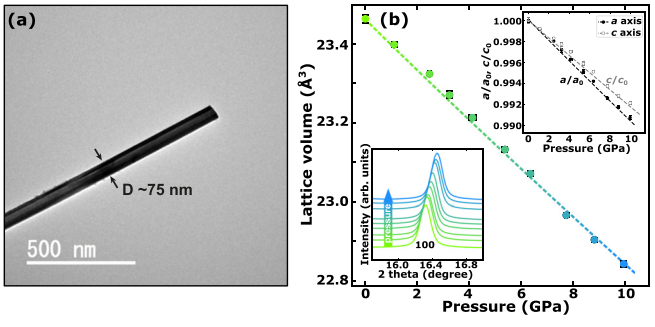

FIG. 3. (a) TEM micrograph of an oxygen-doped TaN NWC. (b) Pressure dependence of the lattice volume of the TaN NWCs. The insets illustrate the shift of the main 100 reflection to higher 2 theta values with increasing pressure (left) and the pressure dependence of the lattice parameter *a* and *c* that are normalized by the lattice parameters at zero-pressure (right). The dashed line represents the fitting to the Birch–Murnaghan equation of state. If error bars are not shown, errors are smaller than the symbols.

(M/H) and the difference between the field cooling (FC) and ZFC curves suggested a superconducting transition at 6.2 K of the NWCs [Fig. S5(b)]. The gradual increase in the FC magnetization data at low temperatures indicated a magnetic phase impurity with a Curie–Weiss-type (CW-type) temperature dependence of the magnetization. Excluding the CW term from the raw data pointed toward typical behavior of usual superconductors. Because the superconducting NaCl-type TaN phase ($T_c \sim 4$–11 K)[55,56] was not detected by synchrotron XRD in the measured sample [Fig. S5(c)], it is strongly suggested that the oxygen-doped TaN NWCs show a superconducting transition at 6.2 K.

Another feature of TM nitrides is a high bulk modulus that is often associated with a high degree of material strength. To receive details about the elasticity of the NWCs, their compression behavior was examined by high-pressure *in situ* synchrotron XRD. Figure 3(b) shows that the lattice volume monotonically decreased with increasing pressure, while the *c* axis possessed less compressibility than the *a* axis. The pressure–volume data were fitted to the Birch–Murnaghan equation of state, which takes the form in its second order,

$$P = \frac{3B_0}{2}\left(\frac{V}{V_0}\right)^{-5/3}\left[\left(\frac{V}{V_0}\right)^{-2/3} - 1\right], \quad (1)$$

with P being the pressure, B_0 being the zero-pressure bulk modulus, and V_0 being the lattice volume at zero pressure. From a least squares fitting, the zero-pressure bulk modulus was derived to 363(6) GPa, which is higher than that of NaCl-type TaN ($B_0 = 295(1)$ GPa), ε-TaN ($B_0 = 318(4)$ GPa), WC-type TaN ($B_0 = 351(4)$ GPa),[39] and Ta_2N_3 ($B_0 = 319(6)$ GPa).[57] This observation indicated an incompressible nature of the NWCs. For details, it is referred to the supplementary material (Table S1 and Fig. S6).

In order to not only clarify the intrinsic physical properties but also grow a larger number of NWCs, the investigation of their growth process and mechanism became of particular interest. No NWC growth had been observed in experiments below the solidus of the ammonium chloride,[58] which supported that the growth strongly depends on the melting of NH_4Cl. Higher synthesis temperatures (e.g., 1300–1400 °C) or shorter heating times (e.g., 5–30 min) did not affect the TaN NWC growth in a significant manner. The details are presented in Fig. S7. For more growth details, starting ε-TaN and NH_4Cl precursors were pre-pressed to pellets and layered in the reaction chamber to survey the boundary between them (Figs. 4 and S8).

The SEM image on a longitudinal section of the recovered sample synthesized at 3 GPa and 1100 °C points toward hexagonal platelet crystals of $Ta_5N_{6-x}O_x$ on the boundary to the starting bulk TaN, followed by a large number of NWCs grown on the layer of the hexagonal crystals [Fig. 4(b)]. Since no hexagonal platelet crystals of the $Ta_5N_{6-x}O_x$ phase were detected in the SEM image [Fig. 4(c)] and XRD pattern of the samples synthesized at 5 GPa and 1100 °C, this phase tends to be unstable at the given *PT* condition. Nonetheless, the presence of oxygen in both synthesis products, oxygen-doped TaN NWCs and $Ta_5N_{6-x}O_x$ crystals, hinted that oxygen contamination played an important role in the NWC growth. The most likely oxygen source was H_2O in the raw NH_4Cl due to its hygroscopic nature.

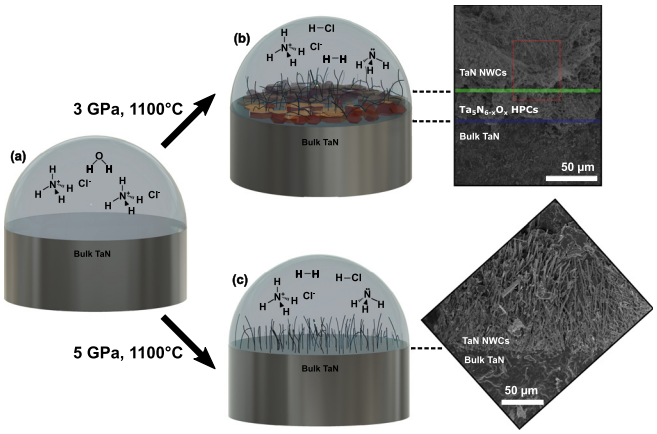

FIG. 4. Simplified illustration of the two-layer cell of the TaN and NH_4Cl (with H_2O) precursor (a) before the chemical reactions to $Ta_5N_{6-x}O_x$ and TaN(O), after growth of (b) hexagonal platelet crystals (HPCs) and nanowire crystals (NWCs) at 3 GPa, 1100 °C (red area: see Fig. S8) and (c) only NWCs at 5 GPa, 1100 °C. Note that the real number of NWCs was several times higher as shown in the SEM images of the respective longitudinal section of the recovered samples.

Therefore, two chemical reactions for the formation of $Ta_5N_{6-x}O_x$ and TaN(O) are given as follows:
Formation of $Ta_5N_{6-x}O_x$

$$5\,\mathrm{TaN} + (1-x)\,\mathrm{NH_4Cl} + x\mathrm{H_2O} \rightarrow \mathrm{Ta_5N_{6-x}O_x} + \frac{3-x}{2}\mathrm{H_2} + (1-x)\mathrm{HCl}. \quad (2)$$

Formation of TaN(O)

$$\mathrm{Ta_5N_{6-x}O_x} \rightarrow 5\mathrm{TaNO_{x/5}} + \frac{1-x}{2}\mathrm{N_2}. \quad (3)$$

After all

$$5\,\mathrm{TaN} + (1-x)\mathrm{NH_4Cl} + x\mathrm{H_2O} \rightarrow 5\mathrm{TaNO_{x/5}} + \frac{1-x}{2}\mathrm{N_2} + \frac{3-x}{2}\mathrm{H_2} + (1-x)\mathrm{HCl} \quad (4)$$

or

$$5\,\mathrm{TaN} + (1-x)\mathrm{NH_4Cl} + x\mathrm{H_2O} \rightarrow 5\mathrm{TaNO_{x/5}} + (1-x)\mathrm{NH_3} + x\mathrm{H_2} + (1-x)\mathrm{HCl}. \quad (5)$$

Indeed, the presence of the minor reaction product HCl was indicated by a short and intense smell immediately after the sample recovery of the high-pressure experiments. The brittle nature of the recovered bulk sample further revealed the gaseous and fluid products during the high P–T treatment. Besides, the longitudinal section SEM images of the recovered samples [Figs. 4(b) and 4(c)] point out a plethora of space and solidified materials among the NWCs. The latter were almost removed by washing the sample in water. These findings support the above-mentioned chemical reactions of the generation of gaseous/fluid materials and imply that the NWCs had been grown in the fluid, i.e., supercritical fluid, or melted material at 3–5 GPa and 1100 °C operating as a solvent flux. Ammonia mixed with hydrogen generated as proposed was able to act as supercritical fluids, whereas the melted material was most likely NH_4Cl. One potential factor for the 1D morphology could be the longitudinal temperature gradient in the reaction chamber induced by the axial extent of the carbon furnace that generated high thermal conduction along the axis of the assembly. Reasons for the morphology of the NWCs remained unclear due to the not entirely elucidated crystal structure at this stage. Also noteworthy is that the nanowire crystals could not be grown in experiments by using Ta and NH_4Cl precursors in which WC-type TaN was synthesized. Finally, the growth experiments were extended to the other ammonium halides (NH_4X with X = I; Br; F), in which the presence of nanowires was confirmed (Fig. S9).

In summary, nanowire crystals of oxygen-doped Ta nitride were fabricated from TaN and NH_4X precursors under GPa-high P–T conditions. They had diameters of ~40–200 nm and lengths of ~100 nm to, in some cases, more than ~50 μm. The oxygen-doped TaN NWC was found to crystallize in the hexagonal crystal structure with a $P6_3/mmc$ space group grown along the crystallographic [001] direction, and SQUID magnetometry suggested a superconducting transition at 6.2 K. Chemical reactions for the growth of the nanowire crystals had been proposed and melted NH_4X in combination with supercritical NH_3 operated as a flux, which significantly controlled the crystal growth. As a result, high-pressure techniques combined with an ammonium halide flux could facilitate unique growth conditions for other 1D nitride-based crystals not accessible at ambient conditions. Further studies are required to understand the growth mechanisms, to determine the atom positions in the crystal structure, and to explore the electronic properties of the nanowire crystals. This could not only promote theoretical investigations on their electronic structure to clarify the reasons for the superconducting transition but also result in the establishment as materials, potentially for electronic applications of the TM nitride nanowire crystals.

See the supplementary material for additional information about high-pressure crystal growth experiments, Scanning and Transmission Electron Microscopy observations, Raman spectroscopy, SQUID magnetometry, and the analysis of the compression behavior.

The authors thank M. Hojamberdiev for helpful discussions. M. Ichikawa, T. Ikoma, R. Fukui, Y. Mori, S. Nomura, K. Kanie, S. Sonntag, and T. Hikage are highly appreciated for technical assistance. Synchrotron x-ray diffraction measurements were conducted with the financial support of the Synchrotron Radiation Research Center, Nagoya University (Proposal Nos. 201902030, 201905051, 2019N2007, 201806051, 2018N5001, and 2018N6001). This research was partially supported by a Grant-in-Aid for Scientific Research from the Ministry of Education, Culture, Sports, Science, and Technology of Japan (Grant Nos. 19H05790 and 16H02388). Z.L., K.N., and M.H. acknowledged partial support from the AIST-Nagoya University Alliance Project.

REFERENCES

[1]A. Friedrich, B. Winkler, L. Bayarjargal, W. Morgenroth, E. A. Juarez-Arellano, V. Milman, K. Refson, M. Kunz, and K. Chen, Phys. Rev. Lett. **105**, 085504 (2010).
[2]J. C. Crowhurst, A. F. Goncharov, B. Sadigh, C. L. Evans, P. G. Morrall, J. L. Ferreira, and A. J. Nelson, Science **311**, 1275 (2006).
[3]A. F. Young, C. Sanloup, E. Gregoryanz, S. Scandolo, R. J. Hemley, and H. K. Mao, Phys. Rev. Lett. **96**, 155501 (2006).

[4]A. Salamat, A. L. Hector, P. Kroll, and P. F. McMillan, Coord. Chem. Rev. **257**, 2063 (2013).
[5]R. Marchand, F. Tessier, and F. J. DiSalvo, J. Mater. Chem. **9**, 297–304 (1999).
[6]X.-J. Chen, V. V. Struzhkin, Z. Wu, M. Somayazulu, J. Qian, S. Kung, A. N. Christensen, Y. Zhao, R. E. Cohen, H-k Mao, and R. J. Hemly, Proc. Natl. Acad. Sci. U. S. A. **102**, 3198–3201 (2005).
[7]U. Patel, S. Avci, Z. L. Xiao, J. Hua, S. H. Yu, and Y. Ito, Appl. Phys. Lett. **91**, 162508 (2007).
[8]M. Shur, Solid State Electron. **155**, 65–75 (2019).
[9]S. Bhattacharyya, J. Phys. Chem. C **119**, 1601–1622 (2015).
[10]S. Wang, D. Antonio, X. Yu, J. Zhang, A. L. Cornelius, D. He, and Y. Zhao, Sci. Rep. **5**, 13733 (2015).
[11]Y. Wang, S.-S. Wang, Y. Lu, J. Jiang, and S. A. Yang, Nano Lett. **16**, 4576 (2016).
[12]F. Wu, C. Huang, H. Wu, C. Lee, K. Deng, E. Kan, and P. Jena, Nano Lett. **15**, 8277 (2015).
[13]S. Wang, H. Ge, S. Sun, J. Zhang, F. Liu, X. Wen, X. Yu, L. Wang, Y. Zhang, H. Xu, J. C. Neuefeind, Z. Qin, C. Chen, C. Jin, Y. Li, D. He, and Y. Zhao, J. Am. Chem. Soc. **137**, 4815 (2015).
[14]A. Zerr, G. Miehe, J. Li, D. A. Dzivenko, V. K. Bulatov, H. Höfer, N. Bolfan-Casanova, M. Fialin, G. Brey, T. Watanabe, and M. Yoshimura, Adv. Funct. Mater. **19**, 2282–2288 (2009).
[15]A. Salamat, K. Woodhead, S. I. U. Shah, A. L. Hector, and P. F. McMillan, Chem. Commun. **50**, 10041 (2014).
[16]A. Salamat, A. L. Hector, B. M. Gray, S. A. J. Kimber, P. Bouvier, and P. F. McMillan, J. Am. Chem. Soc. **135**, 9503 (2013).
[17]A. Zerr, G. Miehe, and R. Riedel, Nat. Mater. **2**, 185–189 (2003).
[18]D. Laniel, A. Dewaele, and G. Garbarino, Inorg. Chem. **57**, 6245–6251 (2018).
[19]M. Bykov, E. Bykova, G. Aprilis, K. Glazyrin, E. Koemets, I. Chuvashova, I. Kupenko, C. McCammon, M. Mezouar, V. Prakapenka, H.-P. Liermann, F. Tasnádi, A. V. Ponomareva, I. A. Abrikosov, N. Dubrovinskaia, and L. Dubrovinsky, Nat. Comm. **9**, 2756 (2018).
[20]V. S. Bhadram, D. Y. Kim, and T. A. Strobel, Chem. Mater. **28**, 1616 (2016).
[21]K. Niwa, K. Suzuki, S. Muto, K. Tatsumi, K. Soda, T. Kikegawa, and M. Hasegawa, Chem. Eur. J. **20**, 13885–13888 (2014).
[22]M. Onodera, F. Kawamura, N. T. Cuong, K. Watanabe, R. Moriya, S. Masubuchi, T. Taniguchi, S. Okada, and T. Machida, APL Mater. **7**, 101103 (2019).
[23]F. Kawamura, H. Yusa, and T. Taniguchi, Appl. Phys. Lett. **100**, 251910 (2012).
[24]S. Wang, X. Yu, Z. Lin, R. Zhang, D. He, J. Qin, J. Zhu, J. Han, L. Wang, H.-K Mao, J. Zhang, and Y. Zhao, Chem. Mater. **24**, 3023 (2012).
[25]S. Fan, X. Feng, Y. Han, Z. Fan, and Y. Lu, Nanoscale Horiz. **4**, 781–788 (2019).
[26]C. Thelander, P. Agarwal, S. Brongersma, J. Eymery, L. F. Feiner, A. Forchel, M. Scheffler, W. Riess, B. J. Ohlsson, U. Gösele, and L. Samuelson, Mater. Today **9**, 28–35 (2006).
[27]Y. Xia, P. Yang, Y. Sun, Y. Wu, B. Mayers, B. Gates, Y. Yin, F. Kim, and H. Yan, Adv. Mater. **5**, 353–389 (2003).
[28]C. Xu, D. He, C. Liu, H. Wang, P. Wang, Q. Wang, and W. Wang, Solid State Sci. **41**, 52–55 (2015).
[29]K. Teshima, K. Yubuta, S. Shimodaira, Y. Fujita, T. Suzuki, M. Endo, T. Shishido, and S. Oishi, Cryst. Growth Des. **2**, 465–469 (2008).
[30]S. Liu, Z.-R. Tang, Y. Sun, J. C. Colmenares, and Y.-J. Xu, Chem. Soc. Rev. **44**, 5053–5075 (2015).
[31]T. Hanrath and B. A. Korgel, Adv. Mater. **15**, 437–440 (2003).
[32]N. D. Zhigadlo, J. Cryst. Growth **382**, 75–79 (2013).
[33]N. D. Zhigadlo, S. Weyeneth, S. Katrych, P. J. W. Moll, K. Rogacki, S. Bosma, R. Puzniak, and J. Karpinski, Phys. Rev. B **86**, 214509 (2012).
[34]K. Watanabe, T. Taniguchi, and H. Kanda, Nat. Mater. **3**, 404–409 (2004).
[35]X. Chen, T. Koiwasaki, and S. Yamanaka, J. Solid State Chem. **159**, 80–86 (2001).
[36]X. Zhao and K.-J. Range, J. Alloys Compd. **296**, 72–74 (2000).
[37]L. G. Boiko and S. V. Popova, JETP Lett. **12**, 101–102 (1970).
[38]D. A. Papaconstantopoulos, W. E. Pickett, B. M. Klein, and L. L. Boyer, Phys. Rev. B **31**, 752 (1985).
[39]H. Yusa, F. Kawamura, T. Taniguchi, N. Hirao, Y. Ohishi, and T. Kikegawa, J. Appl. Phys. **115**, 103520 (2014).
[40]Y. Li, T. Takata, D. Cha, K. Takanabe, T. Minegishi, J. Kubota, and K. Domen, Adv. Mater. **25**, 125–131 (2013).
[41]X. Feng, T. J. LaTempa, J. I. Basham, G. K. Mor, O. K. Varghese, and C. A. Grimes, Nano Lett. **10**, 948–952 (2010).
[42]H. Weng, C. Fang, Z. Fang, and X. Dai, Phys. Rev. B **93**, 241202 (2016).
[43]X. Zhou, P. Jin, S. Chen, and Y. Zhu, Mater. Lett. **136**, 168–170 (2014).
[44]N. Watanabe, T. Nagae, Y. Yamada, A. Tomita, N. Matsugaki, and M. Tabuchi, J. Synchrotron Radiat. **24**, 338–343 (2017).
[45]M. Buchner, K. Höfler, B. Henne, V. Ney, and A. Ney, J. Appl. Phys. **124**, 161101 (2018).
[46]M. A. Garcia, E. Fernandez Pinel, J. de la Venta, A. Quesada, V. Bouzas *et al.*, J. Appl. Phys. **105**, 013925 (2009).
[47]N. Terao, Jpn. J. Appl. Phys., Part 1 **10**, 248 (1971).
[48]J. D. Houmes and H.-C. Zur Loye, J. Solid State Chem. **127**, 267–275 (1996).
[49]H. Schilling, A. Stork, E. Irran, H. Wolff, T. Bredow, R. Dronskowski, and M. Lerch, Angew. Chem., Int. Ed. **46**, 2931–2934 (2007).
[50]Z. Wang, J. Hou, C. Yang, S. Jiao, K. Huang, and H. Zhu, Energy Environ. Sci. **6**, 2134–2144 (2013).
[51]T. Mashimo, S. Tashiro, M. Nishida, K. Miyahara, and E. Eto, Physica B **239**, 13–15 (1997).
[52]B. H. Toby and R. B. Von Dreele, J. Appl. Cryst. **46**, 544–549 (2013).
[53]F. Izumi and K. Momma, Solid State Phenom. **130**, 15–20 (2007).
[54]G. Oszlanyi and A. Suto, Acta Crystallogr., Sect. A **60**, 134–141 (2004).
[55]K. Reichelt, W. Nellen, and G. Mair, J. Appl. Phys. **49**, 5284–5287 (1978).
[56]S. Chaudhuri and I. J. Maasilta, Appl. Phys. Lett. **104**, 122601 (2014).
[57]A. Friedrich, B. Winkler, L. Bayarjargal, E. A. Juarez Arellano, W. Morgenroth, J. Biehler, F. Schröder, J. Yan, and S. M. Clark, J. Alloys Compd. **502**, 5–12 (2010).
[58]C. W. F. T. Pistorius, J. Chem. Phys. **50**, 1436 (1969).